J. Chem. Chem. Eng. 8 (2014) 232-242

Nanometallocarbosilanes: Synthesis, Physicochemical Properties and Structure

Galina Shcherbakova[1*], Pavel Storozhenko[1], Mariya Blokhina[1], Valery Shatunov[1], Denis Sidorov[1], Dmitry Sidorov[1] and Gleb Yurkov[2]

1. SSC RF Federal State Unitary Enterprise "State Research Institute for Chemistry and Technology of Organoelement Compounds", Moscow 105118, Russia

2. A.A. Baikov Institute for Metallurgy and Material Science of Russian Academy of Science, Moscow 119991, Russia

Received: December 24, 2013 / Accepted: January 09, 2014 / Published: March 25, 2014.

Abstract: Highly efficient synthesis methods have been developed and characteristics of nanometallocarbosilanes molecular structure were studied by the research team of GNIIChTEOS (State Research Institute for Chemistry and Technology of Organoelement Compounds). Nanometallocarbosilanes were synthesized by thermal co-condensation of oligocarbosilanes and alkyl amides of refractory metals. Initial, intermediate and final products of side reactions were characterized by ^{1}H, ^{13}C, ^{29}Si NMR (nuclear magnetic resonance), IR (infra-red) spectroscopy, GPC (gel-penetrating chromatography), TGA (thermal gravimetric analysis), TEM (transmission electron microscopy), SEM (scanning electron microscopy), RES (X-ray phase analysis) and elemental analysis. The proposed synthesis method of nanometallocarbosilanes was found to produce fusable soluble organosilicon oligomers with homogeneous distribution of nanoscale (10-20 nm) metal particles in the oligomer matrix. A computational model of the group and elemental composition of nanometallocarbosilanes was developed; it was shown that they are molecular globules of near-spherical shape and rigid polycyclic structure. Thermochemical treatment of nanometallocarbosilanes leads to SiC-nanoceramics (a high yield of up to 75-80 mass%) modified by metal nanoparticles (20-30 nm) contributing to its stabilization. The application of preceramic oxygen-free nanometallocarbosilanes will make it possible to advance in solving the problem of ceramic composite materials with long-term resistance at temperatures above 1,500 °C in oxidizing environments.

Key words: Nanometallocarbosilanes, zirconium, hafnium, tantalum alkyl amides.

1. Introduction

Oxygen-free SiC/SiC composites which are produced on the basis of oxygen-free organosilicon poly(oligo)mers-PCS (polycarbosilanes)—have been currently prioritized for high-duty applications in various branches [1-3].

To create PCS designed for making high-temperature ceramic composites, it has been suggested to modify PCS by introducing various metals into the carbosilane matrix. PCS have been reported to be modified both with metals directly, and with metal organic compounds, with a variety of metals used ranging from aluminum to refractory metals [4-24].

This work results from authors' research dealing with creating oxygen-free preceramic organosilicon oligomers (polymers)—nano-MCS (nanometallo carbosilanes) containing nanoparticles of compounds of refractory metals (Zr, Hf and Ta), which are homogeneously distributed in the final oligomer (polymer) and then, after pyrolysis, in the ceramic matrix as well to form nanoparticles of metal carbides, silicides or nitrides [1-4].

Fiber-forming (or soluble in hydrocarbon solvents) nanometallocarbosilanes can be used not only to form components of ceramic composites (ceramic fibers, matrices, barrier coatings, powders, etc.), but also to

---

[*] **Corresponding author:** Galina Shcherbakova, Dr., research fields: synthesis and structure of organoelement compounds. E-mail: galina7479@mail.ru.

stabilize ultra-thin high-tension ceramics at elevated temperatures. The stabilization mechanism is related to the ability of nanoparticles to slow growth of crystallites at increased temperature and capture oxygen forming inert products [3, 5-7].

2. Experiments

2.1 Materials and Methods

Metal alkyl amides ($Zr[N(C_2H_5)_2]_4$, $Hf[N(CH_3)_2]_4$, $Hf[N(C_2H_5)_2]_4$, $Ta[N(CH_3)_2]_5$), were acquired from OOO “Spektr TT”. The solvents used were acquired from OOO “Component-Reaktiv”. The supplier of PDMS (polydimethylsilane)-$[Si(CH_3)_2]_n$ is Guangdong Agribusiness Group Import and Export Co., Ltd.. OCS (Oligocarbosilanes) were obtained using a technique described in Ref. [27]. Nano-MCS was synthesized by means of thermal co-condensation of OCS and alkyl amides of refractory metals (Zr, Hf and Ta).

All synthesis processes of nano-MCS were performed in dry argon (the content of O_2 and H_2O < 0.005 mass%).

2.2 Physical Measurements

IR (infra-red) spectra of the synthesized samples of nano-MPCS in the form of tablets with KBr were recorded using “Nicolet” iS50R over the range of 400-4,000 cm^{-1} and using Smart iTR™ ATR (attenuated total reflectance) Sampling Accessory (crystal-diamond).

^1H, ^{13}C, ^{29}Si NMR (nuclear magnetic resonance) spectra were taken for solutions of nano-MCS in benzene-D_6 using BRUKER AVANCE-600 NMR spectrometer. The operation frequency in proton is 600.13 MHz, the internal standard is tetramethylsilane.

Molecular weight characteristics of nano-MCS were determined by means of GPC (gel permeation chromatography) using an Agilent 1200 chromatograph with a refractive index detector (Styragel HR1 column, THF as a solvent, column temperature 30 °C, feed rate 1 mL/m, sample volume 50 mcl; calibrated on polystyrene standards prepared by Waters M (peak) = from 580 to 30,000).

TGA (thermogravimetric analysis) of nano-MCS was performed using TGA/SDTA851 Mettler Toledo with heat rate of 10 °C/min in an inert atmosphere (argon) up to 1,100 °C.

Characteristic softening (t_1), fiberization (t_2) and dropping (t_3) temperatures were determined on TMA (thermomechanical analysis) curves using a TMA/SDTA840 Mettler Toledo with heat rate of 10 °C/min. in an inert atmosphere (argon) up to 350 °C.

The pyrolysis of nano-MCS was performed in a Nabertherm 50/500/11 tube furnace in argon with a rate of 5 °C/min up to 1,100 °C and exposure for 1 h to produce ceramic samples.

Metal nanoparticles sizes in nano-MCS samples and ceramic samples, which were obtained as a result of pyrolysis of nano-MCS, were determined by means of TEM (transmission electron microscopy) using a JEOL JEM-1011 microscope accelerating voltage 80 kV).

Surface morphology and the elemental composition of nano-MCS samples and ceramic samples were studied using a JEOL JSM 6380 LA scanning electron microscope (voltage 20 kV) coupled with EDS (energy-dispersive spectroscopy).

The metal content was determined by X-ray fluorescence. The content of carbon and hydrogen was determined using gravimetry by means of burning down the weighed amount in the oxygen flow. The content of nitrogen was determined by Dumas’ method. The content of silicon was determined by spectrophotometry in the form of a silicon-molibdenum complex at wave-length 400 nm.

X-ray phase analysis of the ceramic samples was performed using a Bruker D8 Advance Vario X-ray diffractometer (copper radiation $CuK_{\alpha 1}$) with a Ge monochromator and a Lynx Eye position-sensitive detector, $\theta/2\theta$ geometry, with rotation and using a Bruker D8 Advance X-ray diffractometer (copper radiation $CuK_{\alpha 1}$, $CuK_{\alpha 2}$) with a Goebel mirror, a point detector, $\theta/2\theta$ geometry, with rotation. Data collection was performed using a Bruker DIFFRACplus software package, and analysis was made using such software as EVA, TOPAS and FindIt. Eva analyzed a qualitative composition of the sample using ICDD (International Centre for Diffraction Data) data bases. FindIt allowed searching for CIF files (crystal information file) required for specifying X-ray diffraction patterns of the test samples in TOPAS.

3. Synthesis

3.1 Preparation of Nanozirconiumcarbosilanes and Nanohafniumcarbosilanes

A general route of co-condensation can be described by Scheme 1.

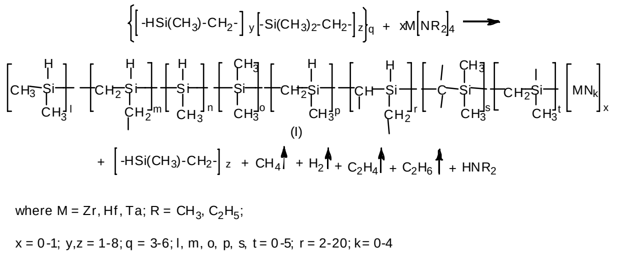

Scheme 1 General route of co-condensation of OCS and alkyl amides of refractory metals (Zr, Hf and Ta).

The process included two stages. At the first stage 25-35 mass% of toluene solution of alkyl amide of a refractory metal (Zr, Hf and Ta) was added to 30-50 mass% OCS in toluene and kept for 1 h while stirring. Then the solvent containing dialkylamine was removed. After the solvent was removed, the reaction mass was kept at 180-185 °C for 0.5 h. Further, the reaction mass was kept under atmospheric pressure at 220 °C for 0.5 h and then at 270-290 °C for 1 h. At the second stage the process was run under residual pressure of 0.2-0.4 kPa, the reaction mass was heated from 20 to 270-290 °C for 2 h and then kept at the set temperature for 1 h with the removal of low-boiling fractions. A fusable nano-MCS with a general route (Scheme 1) soluble in organic solvents was obtained. The metal content in nano-MCS can be controlled from 0.1 to 20.0 mass%. An average molecular weight of nano-MCS according to gel permeation chromatography data was 900-1,500. The dropping temperature ranged from 230 °C to 320 °C.

4. Results and Discussion

4.1 Interaction of Zirconium, Hafnium, Tantalum Alkyl Amides with Oligocarbosilanes

Nanometallocarbosilanes were synthesized by thermal co-condensation of oligocarbosilanes and alkyl amides of refractory metals. Zirconium, hafnium, tantalum alkyl amides are highly soluble in aliphatic and aromatic solvents, are ready to lose their organic framing, and do not contain oxygen and chlorine impurities harmful to the SiC-ceramics. Furthermore, thermal decomposition of Zr, Hf and Ta alkyl amides can result in formation of nitrides and carbonitrides of refractory metals [25], because dissociation energy for D(M–N) bond (Table 1) is higher than that for bonds $D(N{-}CH_3)$ = 211.1 kJ/mol and $D(N{-}C_2H_5)$ = 295.5 kJ/mol.

The formation of high-temperature nitrides and carbonitrides as a result of pyrolysis of preceramic carbosilanes can have a positive effect on properties of the resultant ceramics.

It is important that alkyl amides of refractory metals interact with oligocarbosilanes before the thermal decomposition stage at room temperature in a solvent, and, therefore, the metal is introduced into the oligocarbosilane more gently and completely.

Oligocarbosilanes obtained by thermal rearrangement of PDMS comprise ≡Si–H and $\equiv Si{-}CH_3$ groups, $\equiv Si{-}CH_2{-}Si\equiv$, ≡Si–(CH–)–Si≡ links, as well as residual ≡Si–Si≡ and ≡Si–O–Si≡ links from PDMS (≡Si–O–Si≡ links can form out of ≡Si–OH end group of PDMS). Consequently, when considering possibilities for chemical interaction of alkyl amides of refractory metals and OCS, one should take into

Table 1 M–N bond dissociation energy for alkyl amides of refractory metals.

Compound	D(M–N) (kJ/mol)
$Zr[N(CH_3)_2]_4$	338.7
$Zr[N(C_2H_5)_2]_4$	360.4
$Hf[N(CH_3)_2]_4$	382.5
$Hf[N(C_2H_5)_2]_4$	386.7
$Ta[N(CH_3)_2]_4$	319.5

account first of all reactivity of the above groups. Dissociation energy for bonds D(Si–H) = 334.1 kJ/mol, D(Si–C) = 313.6 kJ/mol, D(Si–O) = 443.2 kJ/mol, D(Si–Si) = 213.3 kJ/mol [26], that is ≡Si–Si≡ bond is the most labile in conditions of thermal decomposition, which is accompanied by its homolytic decomposition. In the present case, however, the reaction begins in the solution at room temperature, so the stronger is ionicity of bonds and groups, the more likely they interact.

The interaction of OCS and tetrakis-(diethylamino) zirconium has been studied in detail [27, 28]. The interaction of $Zr[N(C_2H_5)_2]_4$ with OCS started as low as at room temperature after their solutions were mixed, which was proved by the presence of diethylamine in the reaction mass.

Diethylamine can form as a result of reactions of $Zr[N(C_2H_5)_2]_4$ along the Si–H bond and with end Si–OH groups of OCS. That means even at room temperature some quantity of zirconium is chemically bonded with oligomer molecules of carbosilane. By heating the reaction mass to 60 °C, the resultant diethylamine is removed ($T_{vap.}$ = 55 °C). Further temperature increase to 180 °C can cause thermal destruction of $Zr[N(C_2H_5)_2]_4$ (with detachment of diethylamine and ethylene). Oligomers start to form by hydrosilylation, dehydrocondensation, co-condensation, demethanation and deethanization, which is proved by intense gas evolution observed at 180-200 °C along with removal of the solvent and diethylamine, and at higher temperature accompanied by removal of highly volatile low molecular carbosilanes. Thus, thermal co-condensation of OCS and $Zr[N(C_2H_5)_2]_4$ can be presumed to lead to formation of ZrCS with chemically bonded zirconium. However, the TEM study of ZrCS has showed that a portion of zirconium is in the form of 5-10 nm nanoparticles uniformly distributed across the entire space of the sample and surrounded by a polymer matrix [27, 28].

Co-condensation of OCS with hafnium, tantalum alkyl amides is similar to that of OCS with $Zr[N(C_2H_5)_2]_4$. As a result, metal-containing carbosilanes are formed, they are solid brittle brown products soluble in toluene and hexane.

The resultant metal-containing carbosilanes are X-ray amorphous, but the chemical composition and the main structural links of the oligomer molecule shown in Scheme 1 are confirmed by physical and chemical research data (TEM, ^1H, ^{13}C, ^{29}Si NMR, IR, SEM, GPC, TGA, TMA and elemental analysis).

GPC (MWD), TGA (yield of ceramic residue) and TMA (characteristic temperatures) results are given in Table 2.

Table 2 TGA, TMA and GPC data for nano-MCS.

Exp. No. (M)	*C* (mass%) TGA	Characteristic temperatures (°C)			MWD		
		T_1	T_2	T_3	M_n	M_w	M_w/M_n
1 (Zr)	72.2	250	260	320	830	1,920	2.31
2 (Zr)	73.0	230	245	290	1,400	3,900	2.79
3 (Zr)	67.8	195	205	295	1,070	2,240	2.09
4 (Zr)	74.0	230	240	300	610	950	1.56
5 (Zr)	68.5	155	180	260	620	1,070	1.73
6 (Zr)	75.4	125	150	195	720	1,600	2.22
7 (Zr)	74.3	Not melting			700	2,300	3.29
8 (Zr)	70.6	200	245	315	650	1,550	2.38
9 (Hf)	73.1	160	200	270	970	2,010	2.07
10 (Hf)	65.2	170	215	260	970	1,900	1.95
11 (Hf)	71.0	140	170	230	995	1,880	1.89
12 (Hf)	79.2	180	220	270	1,135	2,350	2.07
13 (Ta)	78.6	210	250	310	1,480	3,640	2.45

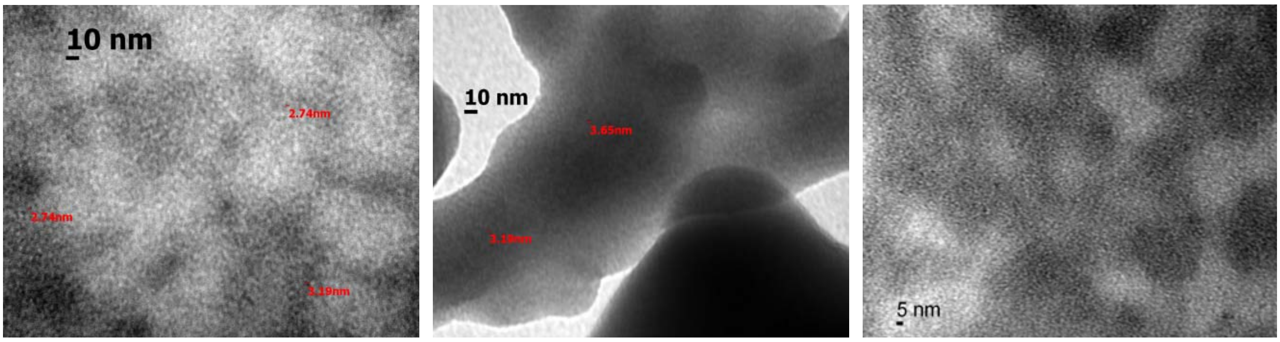

(a) (b) (c)

Fig. 1 TEM of nano-MCS ((a) nano-ZrCS; (b) nano-HfCS; (c) nano-TaCS).

4.2 TEM of Metal-Containing Carbosilanes

Co-condensation of oligocarbosilanes and alkyl amides of refractory metals results in formation of nano-MCS with uniformly distributed metal particles smaller than 10 nm (Fig. 1).

The formation of metal nanoparticles can be explained by a polymerization reaction of alkyl amides of refractory metals, which runs at 200-300 °C in the presence of vapors of alkyl amines to form oligomers (Fig. 2).

A similar reaction is known for tetrakis-(diethylamino) titanium [29]. The formation of metal nanoparticles was studied by TEM of the reaction mass. 10-20 nm metal particles were shown to form in oligomers at the stage of vacuum co-condensation at as low as 285 °C (Fig. 3).

4.3 NMR Spectroscopy

The ^1H NMR spectrum of nano-MCS contains two wide asymmetric signals typical for a spectrum of polycarbosilanes [30]. The first signal centered around 0.3 ppm with two small faint shoulders refers to protons of $SiCH_3$, SiCH and $SiCH_2$ groups. The second one in the area (4.0-5.8 ppm) is caused by a resonance of protons of SiH groups in the various environment. Furthermore, a signal is observed at ~ 2.6 ppm, typical for protons of methyl groups at nitrogen. The ratio of integral intensities of signals is respectively 9-10:1:0.3.

Along with a wide signal at ~3.0 ppm typical for polycarbosilanes, the ^{13}C NMR spectrum of nano-MCS contains a broadened signal at 38.2 ppm, caused by a resonance of carbon atoms of methyl groups bonded to a nitrogen atom.

Three signals are observed in the ^{29}Si NMR spectrum of nano-MCS: The first one in the area of 0.1-0.3 ppm is caused by a resonance of silicon atoms bonded to four carbon atoms of SiC_4, the second one in the area of -16.7 ··· -17.1 ppm belongs to silicon atoms bonded to three carbon atoms and one hydrogen atom of SiC_3H. The third wide minor signal in the

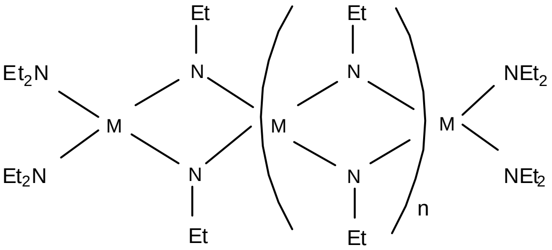

Fig. 2 Polymerization product of alkyl amides of refractory metals.

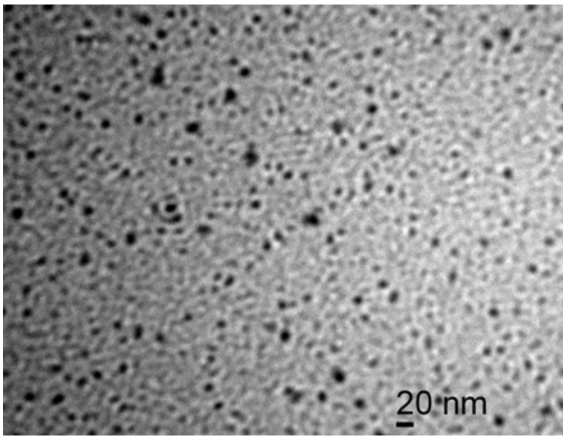

Fig. 3 TEM of nano-MCS (co-condensation at 285 °C).

area of -38 ··· -39 ppm refers to a resonance of silicon atoms in five- and six-membered ring structures. Moreover, there appears a signal at 5.6 ppm in the ^{29}Si spectrum of nano-MCS, which can be referred to a resonance of silicon atoms bonded to a nitrogen atom.

4.4 Infrared Spectroscopy

IR spectra of nano-MCS are observed to have absorption bands in the area of 830, 1,253, 1,406 cm^{-1} (Si–CH$_3$), 1,019 and 1,356 cm^{-1} (Si–CH$_2$–Si), 2,100 cm^{-1} (Si–H), as well as 2,897 and 2,952 cm^{-1} (C–H); similar absorption bands are present in an IR spectrum of any oligo (poly) methylcarbosilane [29]. It should be noted that when a spectrum of nano-MCS in the form of tablets with KBr, unlike carbosilanes, was registered, a wide low-intensity absorption band in the area of 3,435 cm^{-1} (OH) was observed, which is probably related to a higher reactivity of nano-MCS towards oxygen and air moisture as compared with carbosilanes and consequently to H$_2$O vapor holdup from the air while the assay was prepared. When a spectrum was registered using Smart iTR, a universal attachment of single ATR (crystal-diamond), no band was observed in this area, which confirms the above conclusion about a higher reactivity of nano-MCS as compared with carbosilanes.

4.5 SEM/EDS Analysis

A high reactivity of nano-MCS towards oxygen and air moisture explains the presence of oxygen in EDS spectra, when the elemental composition of nano-MCS is determined and the surface relief is studied using SEM. Typical results are given in Fig. 4.

While prepared for SEM analysis, the sample is sputtered with carbon, hence SEM quantitative results show an overstated content of carbon and understated content of the other elements (hydrogen is not detected therewith). It should be noted that nano-MCS samples in air actively absorb oxygen and water vapors, with nano-TaCS being most active, hence EDS spectra register oxygen.

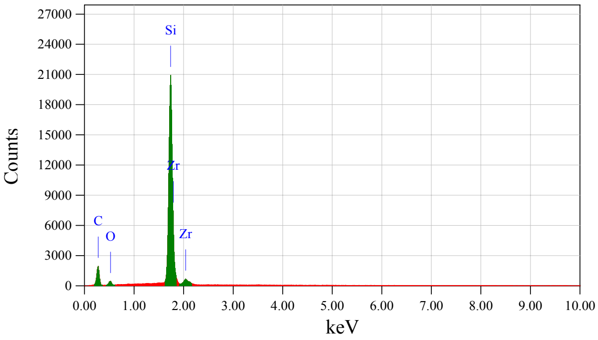

```
ZAF Method Standardless Quantitative Analysis
Fitting Coefficient : 0.1204
Element        (keV)   mass%   Error%    At%
C K            0.277   57.80    0.20   74.94
O K            0.525    6.56    0.32    6.39
Si K           1.739   32.80    0.06   18.18
Zr L           2.042    2.84    0.25    0.49
Total                 100.00          100.00
```

(a)

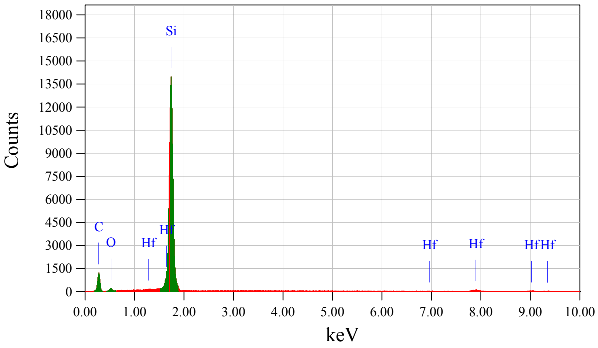

```
ZAF Method Standardless Quantitative Analysis
Fitting Coefficient : 0.1147
Element        (keV)   mass%   Error%    At%
 C K           0.277   55.83    0.14   75.43
 O K           0.525    3.67    0.21    3.73
Si K           1.739   35.26    0.06   20.37
Hf M           1.644    5.24    0.16    0.48
Total                 100.00          100.00
```

(b)

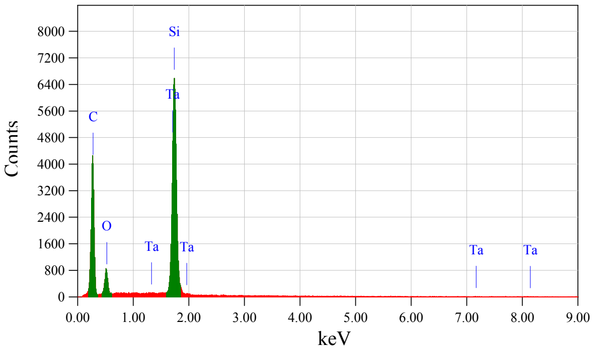

```
ZAF Method Standardless Quantitative Analysis
Fitting Coefficient : 0.2116
Element        (keV)   mass%   Error%    At%
 C K           0.277   69.70    0.11   79.58
 O K           0.525   15.76    0.41   13.51
Si K           1.739   14.07    0.11    6.87
Ta M*          1.709    0.47    0.37    0.04
Total                 100.00          100.00
```

(c)

Fig. 4 SEM/EDS for nano-MCS ((a) nano-ZrCS; (b) nano-HfCS; (c) nano-TaCS).

4.6 Elemental Analysis

The chemical composition of nano-MCS is quantitatively determined by methods of elemental analysis (Table 3).

Empirical formulae of the synthesized nano-MCS (Table 4) were calculated subject to Si/M atomic ratio obtained from experimental data, number-average molecular weight M_n (Table 2) and elemental analysis results (Table 3).

4.7 Molecular Structure Peculiarities of Nano-MCS

Identification of composition and structure of oligo (poly) methylcarbosilanes by elemental analysis, IR spectroscopy and NMR (^{1}H, ^{29}Si and ^{13}C) was supplemented by research made at N. S. Enikolopov ISPM (Institute of Synthetic Polymeric Materials), by GPC, viscometry of dilute solutions and SAXS (small-angle X-ray scattering). The analysis of the data obtained and particularly low values of characteristic viscosity of PCS samples in various solvents against rather high values of molecular weights determined by light scattering data allowed coming to a conclusion about a globular nature of molecular formations of oligo (poly) methylcarbosilanes. Such conclusions agree well with

Table 3 Elemental analysis data for nano-MCS.

Exp. No. (M)	Si-H mass%	Composition of nano-MCS (mass%) (found)					
		C	H	N	Si	M	N/M
1 (Zr)	0.72	37.06	7.83	-	47.34	2.19	-
2 (Zr)	0.57	37.45	7.72	-	44.70	3.18	-
3 (Zr)	0.60	38.95	8.06	1.52	44.83	2.70	3.66
4 (Zr)	0.57	38.35	7.95	2.81	43.05	6.30	2.90
5 (Zr)	0.51	38.69	8.18	2.20	43.48	7.24	1.98
6 (Zr)	0.74	35.92	7.69	0.77	41.31	6.58	0.76
7 (Zr)	-	30.33	6.94	0.81	38.54	17.7	0.30
8 (Zr)	0.57	37.79	7.85	2.56	46.00	4.05	4.10
9 (Hf)	0.67	38.32	7.70	0.94	44.52	3.78	3.16
10 (Hf)	0.61	41.19	8.50	0.61	41.77	3.15	2.47
11 (Hf)	0.57	39.21	8.30	0.48	45.33	3.82	1.60
12 (Hf)	0.58	39.60	8.04	0.55	44.42	3.98	1.76
13 (Ta)	0.62	36.71	8.01	1.04	49.00	5.24	2.53

Table 4 Empirical formulae and calculated composition of nano-MCS.

Exp. No. Empirical formula	Composition of nano-MCS (mass%) (calculated)					
	C	H	N	Si	M	N/M
1. $C_{29.6}H_{76.8}Si_{13.6}Zr_{0.2}$	42.85	9.05	-	45.84	2.17	-
2. $C_{48.6}H_{121.6}Si_{23.2}Zr_{0.5}$	41.67	8.69	-	46.43	3.21	-
3. $C_{35.5}H_{95.7}N_{1.1}Si_{18.15}Zr_{0.3}$	39.70	8.92	1.45	47.36	2.57	3.66
4. $C_{20}H_{46}N_{1.3}Si_{10}Zr_{0.45}$	38.39	7.36	2.91	44.79	6.55	2.89
5. $C_{30.5}H_{54.7}N_{1.0}Si_{14}Zr_{0.5}$	38.98	8.72	2.22	42.86	7.22	2.0
6. $C_{24}H_{54}N_{0.53}Si_{12}Zr_{0.53}$	39.26	7.36	1.01	45.81	6.57	1.0
7. $C_{20}H_{49}N_{0.3}Si_{10}Zr_{1.35}$	34.41	7.02	0.81	40.14	17.6	0.30
8. $C_{22}H_{52}N_{1.2}Si_{11}Zr_{0.3}$	39.51	7.78	2.51	46.10	4.09	4.00
9. $C_{32}H_{84}N_{0.6}Si_{16}Hf_{0.2}$	40.00	8.75	0.87	46.66	3.72	2.98
10. $C_{33}H_{84}N_{0.5}Si_{16}Hf_{0.2}$	40.82	8.66	0.72	46.19	3.68	2.50
11. $C_{34}H_{81}N_{0.45}Si_{16}Hf_{0.3}$	40.88	8.12	0.63	44.89	5.37	1.50
12. $C_{40}H_{103}N_{0.6}Si_{19}Hf_{0.3}$	40.78	8.75	0.71	45.20	4.55	2.00
13. $C_{48}H_{126}NSi_{24}Ta_{0.5}$	38.95	8.52	0.95	45.44	6.12	2.57

SAXS results for dilute solutions of oligo (poly) methylcarbosilanes—a hydrodynamic diameter of spherical globules lies within 1.0-7.6 nm. A good agreement of the hydrodynamic radius and a radius of gyration is evidence of the near spherical shape of molecular globules with a rigid polycyclic structure [31].

Summing up the analytical data one can state that the synthesized nano-MCS are oligomers which consist of three types of molecules:

(1) Molecules, where metal atoms are bonded with carbosilane molecules;

(2) Metal-containing oligomer molecules, where organic ligands are replaced with carbosilane groups;

(3) Molecules of carbosilane oligomers, which do not contain a metal.

Fig. 5 shows a probable structure of nano-MCS (by the example of nano-ZrCS) in consideration of structural formulae suggested earlier for oligomethylcarbosilanes [31].

4.8 Properties of Nano-MPCS Ceramics

Pyrolysis of nano-MPCS in an inert atmosphere was performed to obtain ceramic samples that were explored by TEM, SEM/EDS and X-ray.

Fig. 6 shows the formed 5-10 nm metal particles which are rather uniformly distributed across the entire space of the sample.

SEM/EDS was used to determine an elemental

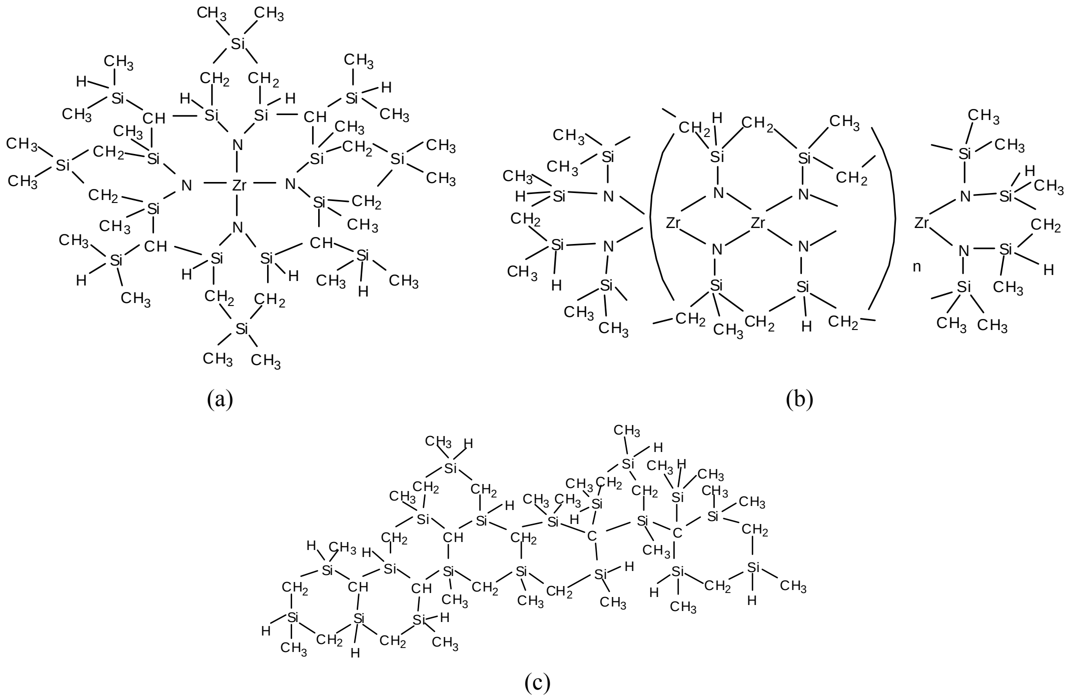
(a) (b) (c)

Fig. 5 A probable structure of nano-ZrCS.

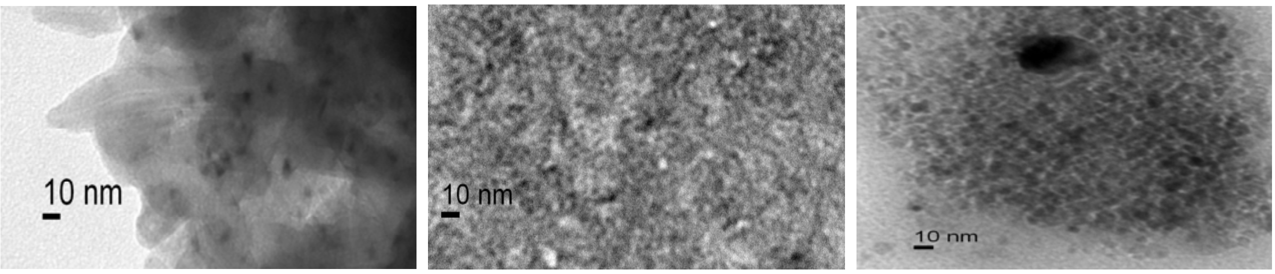

(a) (b) (c)

Fig. 6 TEM image of nano-MCS ceramic samples ((a) nano-ZrCS; (b) nano-HfCS; (c) nano-TaCS).

composition and surface morphology of nano-MCS ceramics (Fig. 7).

SEM results are given for the nano-HfCS ceramic sample taken as an example, with the mapping performed by distribution of elements indicating their uniform distribution (Fig. 8).

X-ray powder diffraction analysis results have shown that nano-ZrCS and nano-HfCS ceramic samples contain silicon carbide as a major phase. The percentage of silicon carbide in these samples is > 99%. Curve 2 (Fig. 9) represents reflections of the silicon carbide phase. The size of crystallites in silicon carbide is D ~ 2 nm.

No known crystalline phases of zirconium and

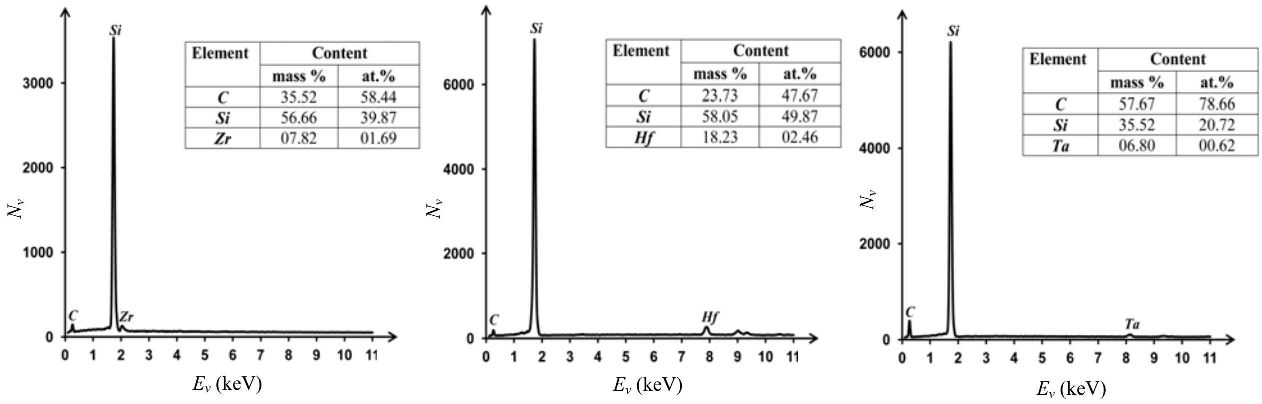

Element	Content	
	mass %	at.%
C	35.52	58.44
Si	56.66	39.87
Zr	07.82	01.69

Element	Content	
	mass %	at.%
C	23.73	47.67
Si	58.05	49.87
Hf	18.23	02.46

Element	Content	
	mass %	at.%
C	57.67	78.66
Si	35.52	20.72
Ta	06.80	00.62

(a) (b) (c)

Fig. 7 SEM/EDS: image of the surface and the elemental composition of nano-MCS ceramic samples.

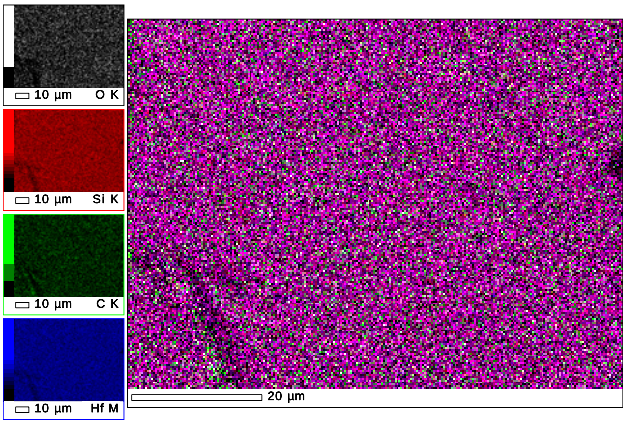

```
ZAF Method Standardless Quantitative Analysis
Fitting Coefficient : 0.1511
Element         (keV)    mass%  Error%      At%
 C K            0.277    44.13    0.41    65.82
 O K            0.525     3.27    0.44     3.65
Si K            1.739    46.85    0.13    29.95
Hf M            1.644     5.75    0.26     0.58
Total                   100.00           100.00
```

Fig. 8 SEM with mapping: image and elemental composition of nano-HfCS ceramics.

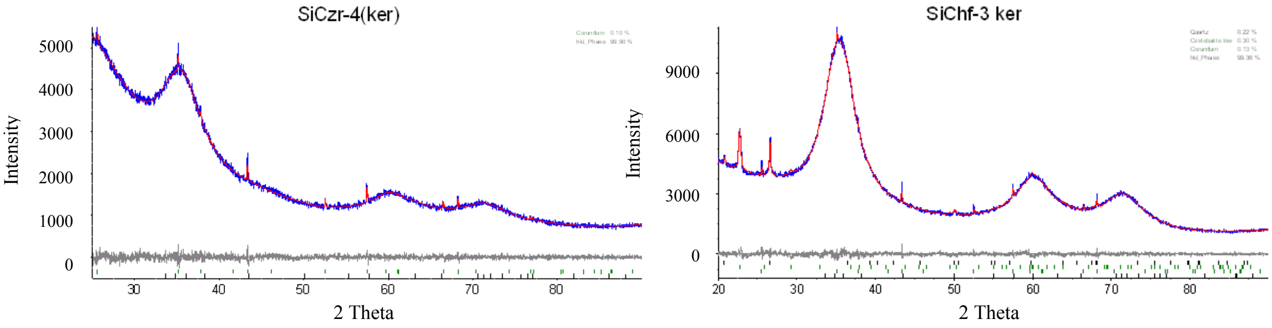

(a) (b)

Fig. 9 XRD patterns of nano-ZrCS (a) and nano-HfCS (b) ceramic samples. Red—calculated curve, blue—experimental curve, grey—difference curve.

hafnium compounds were found in ceramic samples obtained after pyrolysis of nano-ZrCS and nano-HfCS at 1,100 °C. This shows that in the studied samples zirconium and hafnium compounds are in an amorphous state or present in the samples as embedded in the lattice of the major phase. A small size of crystallites of major phases of samples makes this assumption rather logical, because the presence of zirconium and hafnium is confirmed by SEM and X-ray fluorescence analysis data.

5. Conclusions

Co-condensation of oligocarbosilanes and alkyl amides of refractory metals results in formation of fusable soluble organosilicon oligomers with homogeneous distribution of nanoscale metal particles (5-10 nm) in the oligomer matrix. The resultant oligomers are highly capable of fiber- and film-forming from melts or solutions, harden during thermochemical treatment, have a high yield of the ceramic residue in pyrolysis (up to 80 mass%).

Pyrolysis of nano-HfOCS at 1,100 °C has been stipulated to result in formation of nanocrystalline metal-containing ceramics (size of crystallites is D ~ 2 nm).

Acknowledgments

This work was supported by RFBR (project No. 13-03-12014 ofi_m).

The authors are grateful to professor Muzafarov, academician of RAS, for supplementary research that was performed at N. S. Enikolopov ISPM (institute of synthetic polymeric materials).

References

[1] Naslain, R. Materials Design and Processing of High Temperature Ceramic Matrix Composites: State of the Art and Future Trends. *Adv. Compos. Mater.* **1999,** *8,* 3-16.

[2] Tsirlin, A. M.; Shcherbakova, G. I.; Florina, E. K.; Popova, N. A.; Gubin, S. P.; Moroz, E. M.; et al. Nano-Structured Metal Containing Polymer Precursors for High Temperature Non-oxide Ceramics and Ceramic Fibers—Syntheses, Pyrolyses and Properties. *J. Eur. Ceram. Soc.* **2002,** *22,* 2577-2585.

[3] Storozhenko, P. A.; Tsirlin, A. M.; Shcherbakova, G. I.; Florina, E. K. In *Pre-ceramic Polymers for Silicon Carbide Composite Material,* Proceedings of International Workshop "Polymer Materials of the XXI Century", Moscow, Nov. 8-9, 2006.

[4] Xie, Z.; Wang, S.; Chen, Z. Active filler (Aluminum-Aluminum Nitride) Controlled Polycarbosilane Pyrolysis. *J. Inorg. Organomet. Polym.* **2006,** *16*, 69-81.

[5] Huang, X.; Wen, G. Reaction Synthesis of Aluminum Silicon Carbide Ceramics. *Mater. Chem. Phys.* **2006,** *97*, 193-199.

[6] Wen, G. W.; Huang, X. X. Increased High Temperature Strength and Oxidation Resistance of Al_4SiC_4 Ceramics. *J. Eur. Ceram. Soc.* **2006,** *26*, 1281-1286.

[7] Inoue, K.; Yamaguchi, A. Synthesis of Al_4SiC_4. *J. Am. Ceram. Soc.* **2003,** *86*, 1028-1030.

[8] Yamamoto, O.; Ohtani, M.; Sasamoto, T. Preparation and Oxidation of Al_4SiC_4. *J. Mater. Res.* **2002,** *17,* 774-778.

[9] Okuzaki, S.; Iwamoto, Y.; Kondoh, S.; Kikuta, K.; Hirano, S. I. Processing of Silicon Carbide Ceramics Using Chemically Modified Polycarbosilanes. *J. Mater. Res.* **1999,** *14*, 189-195.

[10] Cao, F.; Kim, D. P.; Li, X. D.; Feng, C. X.; Song, Y. C. Synthesis of Polyaluminocarbosilane and Reaction Mechanism Study. *J. App. Polym. Sci.* **2002,** *85*, 2787-2792.

[11] Yu, Y. X.; Li, X. D.; Cao, F.; Feng, C. X. Synthesis and Characterization of Polyaluminocarbosilane as SiC Ceramic Precursor. *Trans. Nonferrous Metals Soc. China.* **2004,** *14*, 641-644.

[12] Yu, Y.; Tang, X. Ceramic Precursor Aluminum-Containing Polycarbosilane: Preparation and Structure. *Inorg. Organomet. Polym.* **2009,** *19*, 389-394.

[13] Greenberg, S.; Clendenning, S. B.; Liu, K.; Manners, I.; Aouba, S.; Ruda, H. E. Synthesis and Lithographic Patterning of Polycarbosilanes with Pendant Cobalt Carbonyl Clusters. *Macromolecules.* **2005,** *38*, 2023-2026.

[14] Chen, Z.; Li, X.; Wang, J.; Wang, G. Study on Polyferrocarbosilane as Precursor of Magnetic Silicon Carbide Ceramic. *Acta Polymerica Sinica.* **2005,** *22*, 535-539.

[15] Popkov, O. V.; Potapova, E. A.; Yurkov, G. Y.; Ovchenkov, E. A.; Shcherbakova, G. I.; Zhigalov, D. V. Magnetic Ceramics Based on Cobalt Ferrite and Silica Nanoparticles Obtained from Polycarbosilane. *Perspectivnye Materialy.* **2012,** *1*, 18-22.

[16] Yajima, S.; Okamura, K.; Hasegawa, Y.; Yamamura, T.

N. Process for Its Production and Shaped Articles of Inorganic Carbide Derived There from. Patent EP 0,030,105, Nov. 21, 1979.

[17] Song, Y.; Feng, C.; Tan, Z.; Lu, Y. Structure and Properties of Polytitanocarbosilane as the Precursor of SiC-TiC Fibre. *J. Mater. Sci. Lett.* **1990,** *9,* 1310-1313.

[18] Kumagawa, K.; Yamaoka, H.; Shibuya, M.; Yamamura, T. Fabrication and Mechanical Properties of New Improved Si-M-C-(O) Tyranno Fiber. *Ceram. Eng. Sci. Proc.* **1998,** *19,* 65-72.

[19] Shaoming, D.; Katoh, Y.; Kohyama, A. Processing Optimization and Mechanical Evaluation of Hot Pressed 2D Tyranno-SA/SiC Composites. *J. Eur. Ceram. Soc.* **2003,** *23,* 1223-1231.

[20] Ishikawa, T.; Kajii, S.; Kohtoku, Y.; Yamamura, T. Structure and Properties of Si-Ti-C-O Fiber-Bonded Ceramics. *Ceram. Eng. Sci. Proc.* **1997,** *18,* 771-778.

[21] Yu, Z.; Zhan, J.; Zhou, C.; Yang, L.; Li, R.; Xia, H. Synthesis and Characterization of SiC(Ti) Ceramics Derived from a Hybrid Precursor of Titanium-Containing Polycarbosilane. *J. Inorg. Organomet. Polym.* **2011,** *21*, 412-420.

[22] Kumagawa, K.; Yamaoka, H.; Shibuya, M.; Yamamura, T. Thermal Stability and Chemical Corrosion Resistance of Newly Developed Continious Si-Zr-C-O Tyranno Fiber. *Ceram. Eng. Sci. Proc.* **1997,** *18,* 113-118.

[23] Babonneau, F.; Soraru, G. D. Synthesis and Characterization of Si-Zr-C-O Ceramics from Polymer Precursors. *J. Eur. Ceram. Soc.* **1991,** *8,* 29-34.

[24] Yang, D.; Yu, Y.; San, H.; Song, Y. Synthesis of Polyyttriocarbosilane and Its Conversion to Yttrium-Containing Ceramic. *J. Inorg. Organomet. Polym.* **2012,** *22*, 731-736.

[25] Baev, A. K.; Mikhailov, V. E. Thermochemistry of Metals Alkyl Amides of Titanium, Vanadium and Chromium Group. *Russian Journal of Physical Chemistry A.* **1989,** *63*, 1713-1724.

[26] Andrianov, K. A. *Methods of Organoelement Chemistry;* Moscow, 1968; pp 11-13.

[27] Storozhenko, P. A.; Shcherbakova, G. I.; Tsirlin, A. M.; Florina, E. K.; Izmailova, E. A.; Savitskii, A. A.; et al. Synthesis of Nanozirconooligocarbosilanes. *Inorganic Materials.* **2006,** *42(10),* 1159-1167.

[28] Shcherbakova, G. I.; Storozhenko, P. A.; Sidorov, D. V.; Blokhina, M. K.; Kuznetsova, M. G.; Polyakova, M. V.; et al. Molecular Structure of Preceramic Nanozirconooligocarbosilanes. *Inorganic Materials.* **2011,** *47(5),* 535-543.

[29] Bürger, H.; Neese, H. J. Titan-Stickstoff-Verbindungen VIII* Thermolyse von Tris(dialkylamino)titan-alkylen. *J. Organomet. Chem.* **1970,** *21,* 381-388.

[30] Yajima, S.; Hasegawa, Y.; Hayash, J.; Iimura, M. Synthesis of Continuous Silicon Carbide Fibre with High Tensile Strength and High Young's Modulus. Synthesis of Polycarbosilane as Precursor. *J. Mater. Sci.* **1978,** *13,* 2569-2576.

[31] Storozhenko, P. A.; Shcherbakova, G. I.; Muzafarov, A. M. Preceramic Carbosilanes: Physicochemical Properties, Molecular Structure Peculiarities. *Nanotechnics* **2009,** *4(20),* 7-13.